Hindawi
Advances in Civil Engineering
Volume 2021, Article ID 6690753, 17 pages
https://doi.org/10.1155/2021/6690753

*Research Article*

# Lateral Parametric Vibration of Footbridge under Pedestrian Excitation considering the Time-Delay Effect

**Zhou Chen**,[1] **Hongxin Lin**,[1] **Deyuan Deng**,[2] **Wanjie Xu**,[3] **Hanwen Lu**,[1] **and Zepeng Chen**[1]

[1]*School of Transportation and Civil Engineering &Architecture, Foshan University, Foshan, China*
[2]*China Construction Steel Engineering Co., Ltd., Shenzhen, Guangdong, China*
[3]*Guangzhou College of Technology and Business, Guangzhou, China*

Correspondence should be addressed to Zhou Chen; gscz19861985@fosu.edu.cn and Hanwen Lu; luhanwen@e.gzhu.edu.cn

Received 14 August 2021; Revised 30 October 2021; Accepted 4 December 2021; Published 23 December 2021

Academic Editor: Wen-Shao Chang



Pedestrian excitation may consequently cause large-scale lateral vibration of the long-span softness of footbridges. Considering the influence of structural geometric nonlinearity, a nonlinear lateral parametric vibration model is established based on the relationship between force and speed. Taking the London Millennium Footbridge as an example, the Galerkin method is applied to formulate parametric vibration equations. In addition, the multi-scale method is used to analyze the parametric vibration of footbridge system theoretically and numerically. The paper aims to find out the reasons for the large-scale vibration of the Millennium Footbridge by calculating the critical number of pedestrians, amplitude-frequency, and phase-frequency characteristics of the Millennium Footbridge during parametric vibration. On the other hand, the paper also studies the influence parameters of the vibration amplitude as well as simulates the dynamic response of the bridge during the whole process of pedestrians on the footbridge. Finally, the paper investigates influences of the time-delay effect on the system parameter vibration. Research shows that: the model established in the paper is reliable; the closer the walking frequency is to two times of the natural frequency, the fewer number of pedestrians are required to excite large vibrations; when the number of pedestrians exceeds the critical number in consideration of nonlinear vibration, the vibration amplitude tends to be stable constant-amplitude vibration, and the amplitude of vibration response is unstable constant-amplitude vibration when only linear vibration is considered; the following factors have an impact on the response amplitude, including the number of pedestrians on footbridge per unit time, damping, initial conditions, and the number of pedestrians in synchronized adjustment. At last, when considering the lag of the pedestrian's force on the footbridge, the time-lag effect has no effect on the amplitude but has an effect on the time needed to reach a stable amplitude.

## 1. Introduction

As application of new materials and requirements for landscape design improves continuously, more and more large-span soft structures are applied in the design and construction of footbridges. For example, the main span of the Millennium Footbridge in London reaches 144 meters [1]. In addition, the main span of S-shaped footbridge in Mianyang of Sichuan Province reaches 200 meters. Therefore, footbridges often exhibit nonlinear vibration including the main resonance, super harmonic resonance, sub-harmonic resonance, and internal resonance under coupling of footbridge caused by pedestrians under pedestrians' dynamic loads. At present, the research on pedestrian-induced pedestrian bridge vibration mainly focuses on linear vibration, whereas few researches on nonlinear vibration have been found. It is therefore necessary to consider and conduct researches on the geometric nonlinearity of footbridges.

Attention has been drawn to the fact that Nakamura considered the situation of pedestrians stopping or slowing down under the condition of large swings. Based on the interaction between pedestrians and footbridges, he proposes a nonlinear change under modal resonance excitation force. Jia established a nonlinear stochastic system of the lateral vibration of the footbridge, and analyzed the stability of the nontrivial solution of the lateral vibration of the

Millennium Footbridge [2]. Blekherman analyzed the London Millennium Footbridge as a double pendulum and studied its nonlinear internal resonance [3]. Subsequently, Blekherman emphasized that autoparametric resonance is the cause of excessive lateral vibration, and based on the double pendulum model, he studied the dynamic interaction between torsional and lateral modes of the steel arc footbridge under the action of harmonic torque [4]. Based on the coupled oscillator theory, Han assumed that the pedestrian's walking frequency followed the Gaussian distribution. So a time-varying nonlinear dynamic equation was developed by using the modal expansion method. More importantly, the author used the model for the study of lateral vibration on the north span of the London Millennium Footbridge [5].

There are few mentioned investigations that consider the geometric nonlinear factors of the structure, but most of them focus on the forced vibration [1, 6–8]. At present, researches on nonlinear parametric vibration basically focus on the suspension cables of stayed cables and suspension bridges [9–11]. In fact, some footbridges will generate excessive lateral vibration under the excitation of pedestrian movement [11–15]. Due to their long span, soft footbridges are generally soft structures with low natural frequencies. The first-order horizontal component of pedestrians' walking frequency ranges between 0.8 and 1.2 Hz, while the frequency of footbridge is beyond this range, and the forced vibration to a large extent cannot induce its large vibration. In parametric vibration, if the excitation frequency is a multiple of the fundamental frequency of the structure, the structure can vibrate greatly. Piccardo has studied the parametric vibration of footbridges and proposed a new mechanism that can trigger excessive lateral vibration when pedestrians cross the bridge [16]. Ouyang proposed a plane pendulum model that can show the change process of the bridge's lateral amplitude. The analysis found that when the lateral frequency of the pedestrian load is twice the lateral natural frequency of the bridge, intense parametric vibration will occur [17]. Based on previous studies, Wang showed that the process of continuous walking can be regarded as a periodic process, which can be expressed in the form of a Fourier series [18]. In order to predict the effect of vertical pedestrian dynamics on footbridges, Bassoli proposed two simulation models to evaluate the structure's response to pedestrian loads [19]. Marcelo combined walking characteristics and footbridges' response data to propose a Biodynamic Synchronized Coupled Model [20]. The current standards for pedestrian-induced footbridge vibration are seriously lacking. The German footbridge design guide EN03 (2007) stipulates that the sensitive range of the lateral first-order frequency of the pedestrian bridge is 0.5–1.2 Hz [21], but it does not consider the case where the lateral first-order frequency of the footbridge is lower than 0.5 Hz. The first-order lateral frequency of the Millennium Bridge is 0.49 Hz, and a large lateral vibration has also occurred. Therefore, the research in this article will play a beneficial role in the improvement of existing standards, and provide guidance for the design and management of footbridges with a first-order transverse frequency less than 0.5 Hz.

Aiming at the large-scale vibration of the low-frequency footbridge, the paper employs a nonlinear parametric vibration model of the footbridge under the loading of pedestrians, in order to reveal the causes for large-scale vibration of low-frequency footbridge. Based on the data measured in the experiment, the relationship between dynamic load coefficient and speed is fitted. Accordingly, in the paper, it models a nonlinear lateral parameter vibration based on the relationship between force and speed. Taking the London Millennium Bridge as an example, the Galerkin approach and the multi-scale perturbation approach has been employed to carry out theoretical and numerical analysis of the large-scale vibration caused by the parametric vibration of footbridge. Meanwhile, this paper further studies the influence of time delay on parametric vibration.

## 2. Nonlinear Parametric Vibration Model of the London Millennium Footbridge

For the beam structure under pedestrian lateral and longitudinal loads, as shown in Figure 1.

The author takes micro-segment where the distance is $x$ from the beam end, assuming that the cross section is perpendicular to the beam axis both before and after deformation. The paper considers the influence of pedestrians distributed on the footbridge to the weight of the footbridge and also noted the impact of crowd to the damping of footbridge. In addition, the author analyzes the force of micro-segment in Figure 1 with elastic mechanics, as shown in Figure 2.

According to the displacement approach [22], the balance equations of longitudinal and lateral movement of micro-segment's centroid are, respectively, expressed as

$$\begin{aligned}\left(\rho_s A + m_{\mathrm{px}}\right)\frac{\partial^2 u}{\partial t^2}\mathrm{d}s + \left(\mu_1 + \rho_c\gamma\right)\frac{\partial u}{\partial t}\mathrm{d}s \\ = \frac{\partial}{\partial s}\left(N\cos\alpha + Q\sin\alpha\right)\mathrm{d}s + f_h\mathrm{d}s,\end{aligned} \tag{1}$$

$$\begin{aligned}\left(\rho A + m_{\mathrm{px}}\right)\frac{\partial^2 w}{\partial t^2}\mathrm{d}s + \left(\mu_2 + \rho_c\gamma\right)\frac{\partial w}{\partial t}\mathrm{d}s \\ = \frac{\partial}{\partial s}\left(N\sin\alpha - Q\cos\alpha\right)\mathrm{d}s + f_l\mathrm{d}s,\end{aligned} \tag{2}$$

where $u(x,t)$ is the longitudinal displacement, $w(x,t)$ is the lateral displacement, $N(x,t)$ is the axial force in the tangential direction of neutral layer after the beam is deformed, $Q(x,t)$ is the shear force, $\rho_s$ is the mass of footbridge's main girder per linear meter, $m_{\mathrm{px}}$ is the mass of pedestrians per linear meter on the footbridge, $\mu_1$ and $\mu_2$ are the vertical and horizontal damping coefficients, respectively, $\rho_c$ is the density of pedestrians' movement on the footbridge, $\gamma$ is the influence coefficient of crowd damping, and $\alpha$ is the section angle. $f_h$ and $f_l$ are the pedestrians' force per meter in the vertical and horizontal directions, which are, respectively, given by

$$\begin{aligned}f_l(t) &= \lambda\alpha_{l1}m_p g\cos\left(\omega_p t\right), \\ f_h(t) &= \lambda\alpha_{h1}m_p g\cos\left(\omega_p t\right) + \lambda\alpha_{h2}m_p g\cos\left(\omega_p t\right) \\ &= \lambda\sqrt{\alpha_{h1}^2 + \alpha_{h2}^2}\,m_p g\sin\left(\omega_p t - \arctan\frac{\alpha_{h2}}{\alpha_{h1}}\right).\end{aligned} \tag{3}$$

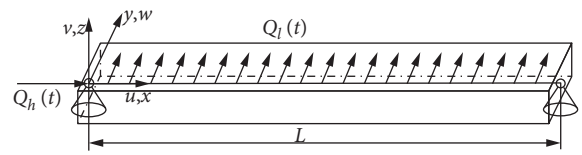


Figure 1: Force analysis on micro-segment of beam under longitudinal and lateral loading.

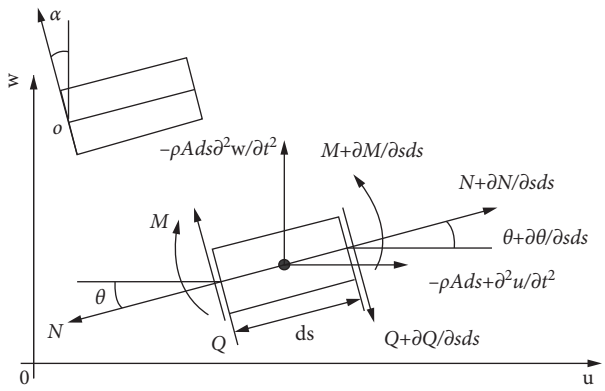


Figure 2: Force analysis on beam and micro-segment under longitudinal and lateral loading by pedestrians.

In which, $\alpha_{l1}$ is the first-order lateral dynamic load coefficient, $\alpha_{ls}$ is the pedestrian dynamic load coefficient related to footbridge vibration, which is related to pedestrians and bridges, whereas the values of coefficient will vary under the condition of different pedestrians and footbridge. $\alpha_{h1}$ is the first-order longitudinal dynamic load coefficient, $\alpha_{h2}$ is the second-order longitudinal dynamic load factor, and $\omega_p$ is the pedestrian walking frequency in the vertical and horizontal directions. In addition, $\lambda$ stands for pedestrians' synchronous adjustment ratio, by ignoring the pedestrians' dynamic load coefficient concerning the footbridge vibration.

Regardless of the influence of the beam's rotation, the shear force $Q(x,t)$ and the bending moment $M(x,t)$ meet to form the following relationship, which can be expressed as

$$Q = \frac{\partial M}{\partial s} = \cos\,\alpha \frac{\partial M}{\partial x}. \tag{4}$$

When equation (4) is substituted into equations (1) and (2) to obtain equation (5) and equation (6) as

$$\begin{aligned}&\left(\rho A + m_p\right)\frac{\partial^2 u}{\partial t^2} + \left(\mu_1 + \rho_c \gamma\right)\frac{\partial u}{\partial t}\\ &\quad = \frac{\partial}{\partial x}\left(N\,\cos\,\alpha + \frac{\partial M}{\partial x}\cos\,\alpha\,\sin\,\alpha\right)\cos\,\alpha + f_h(t),\end{aligned} \tag{5}$$

$$\begin{aligned}&\left(\rho A + m_p\right)\frac{\partial^2 w}{\partial t^2} + \left(\mu_2 + \rho_c \gamma\right)\frac{\partial u}{\partial t}\\ &\quad = \frac{\partial}{\partial x}\left(N\,\sin\,\alpha - \frac{\partial M}{\partial x}\cos^2\,\alpha\right)\cos\,\alpha + f_l(t).\end{aligned} \tag{6}$$

According to the deformation of beam, maintaining the second-order truncation, it can get:

$$\begin{aligned}\sin\,\theta &= \frac{\partial w}{\partial x},\\ \cos\,\theta &\approx 1.\end{aligned} \tag{7}$$

Based on the assumption of equation (7), the axial force and bending moment are obtained by integrating on the cross section of the beam, which are given by

$$\begin{aligned}N(x,t) &= \iint \sigma(x,z,t)\mathrm{d}A\\ &= E\iint\left\{\frac{\partial u(x,t)}{\partial x} + \frac{1}{2}\left[\frac{\partial w(x,t)}{\partial x}\right]^2\right\}\cos\,\theta(x,t)\mathrm{d}A\\ &= \mathrm{EA}\left[\frac{\partial u}{\partial x} + \frac{1}{2}\left(\frac{\partial w}{\partial x}\right)^2\right],\end{aligned} \tag{8}$$

$$\begin{aligned}M(x,t) &= \iint \sigma(x,z,t) z\mathrm{d}A\\ &= E\iint z\left\{\frac{\partial u(x,t)}{\partial x} + \frac{1}{2}\left[\frac{\partial w(x,t)}{\partial x}\right]^2\right\}\cos\,\theta(x,t)\mathrm{d}A\\ &= \mathrm{EI}\frac{\partial \theta}{\partial x}.\end{aligned} \tag{9}$$

Substituting $\partial w/\partial x = \tan\,\theta$ into equation (9) leads to bending moment, which is given by

$$M(x,t) = \mathrm{EI}\frac{\partial^2 w}{\partial x^2}\cos^2\,\theta. \tag{10}$$

To take the second-order truncation, therefore, it is given by

$$\cos\,\theta \approx 1 - \left(\frac{\partial w}{\partial x}\right)^2. \tag{11}$$

If equations (10) and (11) are inserted into equations (5) and (6) to obtain a dynamic equation with only unknown displacements in the vertical and horizontal directions, as

$$\begin{aligned}&\left(\rho A + m_{\mathrm{px}}\right)\frac{\partial^2 u}{\partial t^2} + \left(\mu_1 + \rho_c \gamma\right)\frac{\partial u}{\partial t}\\ &\quad = \mathrm{EA}\frac{\partial^2 u}{\partial x^2} + \mathrm{EA}\frac{\partial w}{\partial x}\frac{\partial^2 w}{\partial x^2} + \mathrm{EI}\frac{\partial^4 w}{\partial x^4}\frac{\partial w}{\partial x} + \mathrm{EI}\frac{\partial^3 w}{\partial x^3}\frac{\partial^2 w}{\partial x^2}\\ &\qquad - 7\mathrm{EI}\frac{\partial^3 w}{\partial x^3}\frac{\partial^2 w}{\partial x^2}\left(\frac{\partial w}{\partial x}\right)^2 - 4\mathrm{EI}\left(\frac{\partial^2 w}{\partial x^2}\right)^3\frac{\partial w}{\partial x} + f_h(t),\end{aligned} \tag{12}$$

$$\begin{aligned}&\left(\rho A + m_{\mathrm{px}}\right)\frac{\partial^2 w}{\partial t^2} + \left(\mu_2 + \rho_c \gamma\right)\frac{\partial w}{\partial t} + \mathrm{EI}\frac{\partial^4 w}{\partial x^4}\\ &\quad = \mathrm{EA}\frac{\partial^2 u}{\partial x^2}\frac{\partial w}{\partial x} + \mathrm{EA}\frac{\partial u}{\partial x}\frac{\partial^2 w}{\partial x^2} + \frac{3}{2}\mathrm{EA}\left(\frac{\partial w}{\partial x}\right)^2\frac{\partial^2 w}{\partial x^2}\\ &\qquad + \mathrm{EI}\frac{\partial^4 w}{\partial x^4}\left(\frac{\partial w}{\partial x}\right)^2 + 6\mathrm{EI}\frac{\partial^3 w}{\partial x^3}\frac{\partial^2 w}{\partial x^2}\frac{\partial w}{\partial x}\\ &\qquad + 2\mathrm{EI}\left(\frac{\partial^2 w}{\partial x^2}\right)^3 + f_l(t),\end{aligned} \tag{13}$$

where equations (12) and (13) are coupled dynamic equations in the vertical and horizontal directions after taking into account the geometric nonlinear effects of footbridge. Since the longitudinal stiffness of beam is much greater than the lateral stiffness, the longitudinal and lateral coupled vibration of the beam is not considered, that it is to say, by ignoring the effect of beam's lateral movement on its longitudinal motion, in this case, equation (12) becomes a linear vibration equation, which is given by

$$\left(\rho A + m_{\mathrm{px}}\right)\frac{\partial^2 u}{\partial t^2} + \left(\mu_1 + \rho_c \gamma\right)\frac{\partial u}{\partial t} - \mathrm{EA}\frac{\partial^2 u}{\partial x^2} = f_h. \tag{14}$$

Regardless of the longitudinal inertia of the beam, the axial force is given by:

$$N(x,t) = \mathrm{EA}\frac{\partial u}{\partial x} = -f_h l \Rightarrow \frac{\partial N}{\partial x} = \mathrm{EA}\frac{\partial^2 u}{\partial x^2} = 0. \tag{15}$$

In this way, equation (13) can be rewritten as:

$$\begin{aligned}&\left(\rho A + m_{\mathrm{px}}\right)\frac{\partial^2 w}{\partial t^2} + \left(\mu_2 + \rho_c \gamma\right)\frac{\partial w}{\partial t} + \mathrm{EI}\frac{\partial^4 w}{\partial x^4}\\ &\quad = \mathrm{EA}\frac{\partial^2 u}{\partial x^2}\frac{\partial w}{\partial x} + \mathrm{EA}\frac{\partial u}{\partial x}\frac{\partial^2 w}{\partial x^2} + \frac{3}{2}\mathrm{EA}\left(\frac{\partial w}{\partial x}\right)^2\frac{\partial^2 w}{\partial x^2}\\ &\qquad + \mathrm{EI}\frac{\partial^4 w}{\partial x^4}\left(\frac{\partial w}{\partial x}\right)^2 + 6\mathrm{EI}\frac{\partial^3 w}{\partial x^3}\frac{\partial^2 w}{\partial x^2}\frac{\partial w}{\partial x}\\ &\qquad + 2\mathrm{EI}\left(\frac{\partial^2 w}{\partial x^2}\right)^3 + f_l(t).\end{aligned} \tag{16}$$

Therefore, by virtue of equation (16), we can obtain a nonlinear parametric vibration equation which considers the pedestrian's influence on the mass and damping of footbridge.

## 3. Lateral Nonlinear Vibration Analysis of Mid-Span of the London Millennium Bridge

*3.1. Project Overview.* The London Millennium Footbridge is a flexible suspension footbridge with a neoteric structure built on the Thames River in London, with a span combination of 81 + 144 + 108 m. Nearly 100,000 people walked across the footbridge on the opening day, and up to 2,000 people were walking on the footbridge. The crowd density was about 1.4 people/m$^2$. A large number of pedestrians caused problems of large lateral vibration. The first-order lateral frequency of mid-span on the footbridge is lower than 0.5 Hz, while the second-order frequency is lower than 1.0 Hz. It is worth noting that the fundamental frequency is not within the range of pedestrian's lateral walking frequency. According to on-site visual observation, the maximum lateral acceleration of the mid-span bridge is estimated to be 2 m/s$^2$–2.5 m/s$^2$. In the paper, it simplifies the London Millennium Footbridge, takes its equivalent stiffness, and calculates equivalent section. Figure 3 shows the Millennium Bridge in London.

Since the author basically attempts to explain the causes for large lateral vibration of the London Millennium Bridge from the perspective of parametric vibration, if the second-order factor is taken into consideration, then it is forced vibration. Besides, the second-order frequency is beyond the range of lateral swing frequency when pedestrians are walking normally. In that case, only considering the first-order mode, it is supposed that the first-order mode function is $\phi(x) = \sin(\pi x/L)$, and the solution of equation (17) reads as:

$$w(x,t) = w_1(t)\sin\frac{\pi x}{l}. \tag{17}$$

Here, $w_1(t)$ presents the generalized coordinates of the first-order mode shape. Substituting equation (17) into equation (16), we employ the Galerkin approach to discretize it, and finally obtain the single-mode vibration differential equation of the Millennium Footbridge by taking the influence of the crowd on the footbridge's quality into consideration, so that it meets with the following equation:

$$\begin{aligned}&\ddot{w}_1(x,t) + \widehat{\zeta}_1\dot{w}_1(x,t) + \omega_1^2 w_1(x,t)\\ &\quad - \widehat{\beta}_1 w_1(x,t)\cos\left(\omega_p t\right) + \widehat{\beta}_2 w_1^3(x,t) - \widehat{F}_0\cos\left(\omega_p t\right) = 0,\end{aligned} \tag{18}$$

where

Figure 3: London Millennium Bridge looking north [23].

$$\begin{aligned}
\widehat{\zeta}_1 &= 2\zeta_0\omega_1,\\
\omega_1 &= \sqrt{\frac{\mathrm{EI}\pi^4}{l^4\left(\rho A + m_p\right)}},\\
\widehat{\beta}_1 &= \frac{\pi^2 l^2 \lambda \alpha_{h1} m_p g}{l^4\left(\rho A + m_p\right)},\\
\widehat{\beta}_2 &= \frac{10\mathrm{EI}\pi^6 + 3\pi^4 l^2 \mathrm{EA}}{8l^6\left(\rho A + m_p\right)},\\
\widehat{F}_0 &= \frac{4\lambda\alpha_{l1} m_p g}{\pi\left(\rho A + m_p\right)},
\end{aligned} \tag{18a, 18b}$$

where $\omega_1$ is the frequency of the footbridge structure on account of the influence of crowd quality. It is related to the number of pedestrians on the footbridge. Given that pedestrians will exert vertical and horizontal harmonic effects on footbridge during the walking process, the longitudinal harmonic forces show parametric excitations on the vibration of footbridge, such as the fourth term in equation (18). However, due to the limitation of pedestrian load, the parametric excitation of longitudinal load is considerably weak.

On the basis of the data measured by Piccardo [16], the relationship between dynamic load coefficient and speed is obtained by fitting the test data, as shown in Figure 4. From Figure 4, it can be seen that the dynamic load coefficient has a linear relationship with speed. Meanwhile, the lateral movement of pedestrians is harmonic motion, and therefore it is found as:

$$f_l(t) = \lambda\left[\alpha_{l1} + \alpha_{lv}\frac{\partial w(x,t)}{\partial t}\right] m_p g\,\cos\left(\omega_p t\right), \tag{19}$$

where $\alpha_{l1}$ is regarded as the dynamic load factor of the pedestrian on the fixed platform, and $\alpha_{lv}$ is the dynamic load factor related to the lateral speed of the footbridge. Different bridges have different values, and different $\alpha_{lv}$ will cause different amplitudes of the footbridge. According to the result of curve fitting, $\alpha_{l1} = 0.04$ and $\alpha_{lv} = 0.7$.

*3.2. Approximate Solution of Parametric Resonance.* The multi-scale approach is employed to solve equation (18). Since the pedestrian excitation frequency is not close to $\omega_1$, small parameters are applied into the damping term, parametric excitation term, and nonlinear term, and the following scaling transformations are given by

$$\begin{aligned}
&0 \le \varepsilon \ll 1,\\
&\widehat{\zeta}_1 = \varepsilon\zeta_1,\\
&\widehat{\beta}_1 = \varepsilon\beta_1,\\
&\widehat{\beta}_2 = \varepsilon\beta_2,\\
&\mu = O(1).
\end{aligned} \tag{20}$$

Combining the abovementioned equations with equation (19), it can be rewritten as

$$\begin{aligned}
&\ddot{w}_1(t) + \varepsilon\zeta_1\dot{w}_1(t) - \varepsilon\zeta_2\cos\left(\omega_p t\right)\dot{w}_1(t)\\
&\quad + \omega_1^2 w_1(t) - \varepsilon\beta_1\cos\left(\omega_p t\right)w_1(t)\\
&\quad + \varepsilon\beta_2 w_1^3(t) - \varepsilon F_0\cos\left(\omega_p t\right) = 0.
\end{aligned} \tag{21}$$

In equation (21) $\widehat{\zeta}_2 = \varepsilon\zeta_2$ and $\zeta_2 = \lambda\alpha_{lv} m_p g/(\rho A + m_p)$ caused by the vibration speed of the footbridge, the third term presents parametric vibration, which is induced by the force from the crowd's movement on the footbridge. Furthermore, the fifth term shows the parametric vibration generated by the pedestrian's longitudinal load, and the seventh term is the forced vibration of pedestrians' walking.

The time scales are adopted as $T_0 = \tau$ and $T_1 = \varepsilon\tau$. The first approximate solution of equation (21) is then given by:

$$w_1(t) = u_0(T_0, T_1) + \varepsilon u_1(T_0, T_1). \tag{22}$$

Differential operators of partial derivatives are expressed as

$$\frac{d}{\mathrm{d}t} = \sum_{r=0}^{+\infty}\frac{\mathrm{d}T_r}{\mathrm{d}t}\frac{\partial}{\partial T_r} = \sum_{r=0}^{+\infty}\varepsilon^r\frac{\partial}{\partial T_r} \overset{\text{def}}{=} \sum_{r=0}^{+\infty}\varepsilon^r D_r, \tag{23}$$

$$\begin{aligned}
\frac{d^2}{\mathrm{d}t^2} &= \sum_{r=0}^{+\infty}\varepsilon^r D_r\left(\sum_{s=0}^{+\infty}\varepsilon^s D_s\right)\\
&= D_0^2 + 2\varepsilon D_0 D_1 + \varepsilon^2\left(D_1^2 + 2D_0 D_2\right) + \cdots,
\end{aligned} \tag{24}$$

where $D_r = \partial/\partial T_r$, $D_r^2 = \partial^2/\partial T_r^2$, $D_n\,(n = 1, 2, 3\cdots m)$. Equations (22) and (24) are inserted into equation (21), and it is assumed that, equalizing the coefficients of the small parameters on both sides of the equation, the following linear partial differential equations can be obtained as

$$\varepsilon^0:\ D_0^2 u_0 + \omega_1^2 u_0 = 0, \tag{25}$$

$$\begin{aligned}
\varepsilon^1:\ D_0^2 u_1 + \omega_1^2 u_1 &= -2D_0 D_1 u_0 - \zeta_1 D_0 u_0 + \zeta_2 D_0 u_0\cos\left(\omega_p t\right)\\
&\quad + \beta_1\cos\left(\omega_p t\right)u_0 - \beta_2 u_0^3 + F_0\cos\left(\omega_p t\right).
\end{aligned} \tag{26}$$

Then, the solution of equation (25) is obtained as

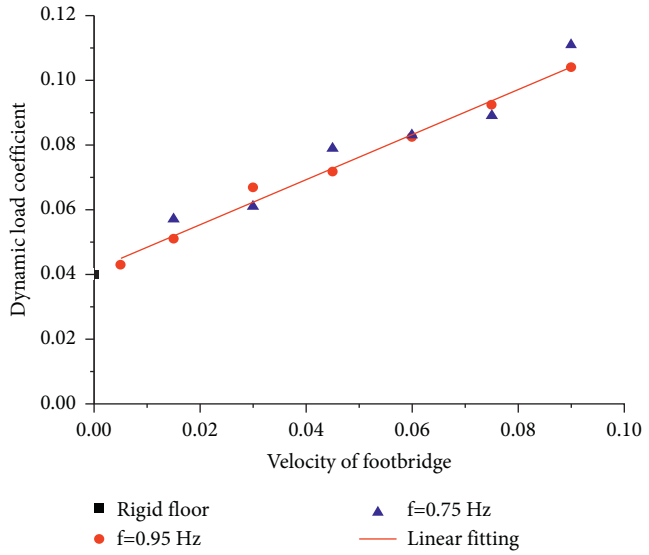


Figure 4: Relationship between dynamic load factor and speed [16].

$$u_0(T_0, T_1) = A(T_1)e^{j\omega_1 T_0} + \overline{A}(T_1)e^{-j\omega_1 T_0}. \tag{27}$$

$\zeta_2 D_0 u_0 \cos(\omega_p t)$, $\beta_1 \cos(\omega_p t) u_0$, and $F_0 \cos(\omega_p t)$ are rewritten into plural form $0.5\zeta_2 D_0 u_0 e^{j\omega_p T_0} + \text{cc}$, $0.5\beta_1 u_0 e^{j\omega_p T_0}$, and $0.5F_0 e^{j\omega_p T_0} + \text{cc}$. Furthermore, equation (27) is substituted into equation (26) to be given by

$$\begin{aligned} D_0^2 u_1 + \omega_1^2 u_1 = &-(2D_1 A j\omega_1 + \zeta_1 A j\omega_1)e^{j\omega_1 T_0} \\ &+ \frac{\zeta_2 j\omega_1}{2}\left(Ae^{j(\omega_p+\omega_1)T_0} - \overline{A}e^{j(\omega_p-\omega_1)T_0}\right) \\ &+ \frac{\beta_1}{2}\left(Ae^{j(\omega_p+\omega_1)T_0} + \overline{A}e^{j(\omega_p-\omega_1)T_0}\right) \\ &- \beta_2\left(A^3 e^{3j\omega_1 T_0} + 3A^2\overline{A}e^{j\omega_1 T_0}\right) \\ &+ \frac{F_0}{2}e^{j\omega_p T_0} + \text{cc}, \end{aligned} \tag{28}$$

where cc is the conjugate complex number of the previous equation. It can be seen from equation (28) that, if $\omega_p \approx 2\omega_1$, there will be parametric resonance in the system, while if $\omega_p \approx \omega_1$, it will generate forced vibration in the system. Here, we generally study the first-order modal vibration of the London Millennium Footbridge. On this basis, the interaction of parameters and forced vibration is analyzed in the following, when $\omega_p \approx 2\omega_1$:

A new excitation frequency tuning parameter is inserted into the equation, and supposing that

$$\omega_p = 2\omega_1 + \varepsilon\sigma. \tag{29}$$

In virtue of equation (28), the conditions for eliminating the permanent term can be given by

$$\begin{aligned} &2D_1 A j\omega_1 + \zeta_1 A j\omega_1 + \frac{\zeta_2 j\omega_1}{2}\overline{A}e^{j\sigma T_1} \\ &-\frac{\beta_1}{2}\overline{A}e^{j\sigma T_1} + 3\beta_2 A^2\overline{A} = 0, \end{aligned} \tag{30}$$

$A(T_1)$ is rewritten in exponential form as

$$A(T_1) = \frac{a_1(T_1)}{2}e^{j\gamma_1(T_1)}. \tag{31}$$

Substituting equation (31) into (30), comparing its real part and imaginary parts, and $\psi$ is assigned a fixed value, $\psi = \sigma T_1 - 2\gamma_1$, then it is easily found that

$$D_1 a_1 = -\frac{\zeta_1 a_1}{2} - \frac{\zeta_2 a_1}{4}\cos\varphi - \frac{\beta_1 a_1}{4\omega_1}\sin\varphi, \tag{32}$$

$$D_1\varphi_1 = \sigma + \frac{\zeta_2}{2}\sin\varphi - \frac{\beta_1}{2\omega_1}\cos\varphi - \frac{3\beta_2 a_1^2}{4\omega_1}. \tag{33}$$

When $D_1 a_1 = 0$ and $D_1\varphi_1 = 0$,

$$\zeta_1 = -\frac{\zeta_2}{2}\cos\varphi - \frac{\beta_1}{2\omega_1}\sin\varphi, \tag{34}$$

$$\sigma - \frac{3\beta_2 a_1^2}{4\omega_1} = \frac{\beta_1}{2\omega_1}\cos\varphi - \frac{\zeta_2}{2}\sin\varphi. \tag{35}$$

The sum of squares of equations (34) and (35) can be given by

$$\zeta_1^2 + \left(\sigma - \frac{3\beta_2 a_1^2}{4\omega_1}\right)^2 = \frac{\beta_1^2}{4\omega_1^2} + \frac{\zeta_2^2}{4}. \tag{36}$$

Equation (36) presents the amplitude-frequency curve of the nonlinear parametric vibration on the Millennium Footbridge. To solve equations (34) and (35), the phase is found as

$$\tan\varphi = \frac{4\omega_1\zeta_1\beta_1 + 4\zeta_2\omega_1\left(4\omega_1\sigma - 3\beta_2 a_1^2\right)}{4\omega_1^2\zeta_1\zeta_2 - \left(4\omega_1\sigma - 3\beta_2 a_1^2\right)\beta_1}. \tag{37}$$

To solve equation (36), it gives

$$a_1 = \pm\sqrt{\frac{4\omega_1\sigma}{3\beta_2} \pm \frac{4\omega_1}{3\beta_2}\sqrt{\frac{\beta_1^2}{4\omega_1^2} + \frac{\zeta_2^2}{4} - \zeta_1^2}}. \tag{38}$$

In order to investigate the stability of equations (32) and (33) in nontrivial solutions, the microtorsion methodology is employed to assume that

$$\begin{aligned} a_n &= a_1 + \Delta a_1, \\ \varphi_n &= \varphi_1 + \Delta\varphi_1, \end{aligned} \tag{39}$$

where $\Delta a_1$ and $\Delta\varphi_1$ represent tiny torsion momentum. Substituting equation (39) into and equations (32) and (33) lead to

$$D_1\Delta a_1 = -\frac{\zeta_1\Delta a_1}{2} - \frac{\zeta_2\Delta a_1}{4}\cos\varphi_1 + \frac{\zeta_2 a_1}{4}\sin\varphi_1\Delta\varphi - \frac{\beta_1\Delta a_1}{4\omega_1}\sin\varphi\frac{\beta_1 a_1}{4\omega_1}\cos\varphi_1\Delta\varphi, \quad (40)$$

$$D_1\Delta\varphi_1 = \frac{\zeta_2}{2}\cos\varphi_1\Delta\varphi + \frac{\beta_1}{2\omega_1}\sin\varphi_1\Delta\varphi - \frac{3\beta_2 a_1\Delta a_1}{2\omega_1}.$$

By considering equations (34) and (35), and eliminating $\sin\varphi_1$ and $\cos\varphi_1$, the characteristic equation is easily obtained as

$$\lambda^2 + \nu_1\lambda + \chi_1 = 0, \quad (41)$$

with

$$\nu_1 = \zeta_1, \quad (42a)$$

$$\chi_1 = \frac{a_1}{2}\left(\sigma - \frac{3\beta_2 a_1^2}{4\omega_1}\right)\frac{3\beta_2 a_1}{2\omega_1}. \quad (42b)$$

Assuming $\nu_1 = \zeta_1 > 0$, then, when $X_1 > 0$, its nontrivial solution is stable; otherwise, it is unstable.

*3.3. Critical Conditions for Parametric Vibration of the Millennium Footbridge.* Since the parametric vibration can only occur under certain conditions, the conditions that affect parametric vibration of the London Millennium Footbridge are basically damping and the number of pedestrians' movement on the footbridge. The critical condition is determined by the solvability of response amplitude. By virtue of the response amplitude $a_1$ being real numbers, then $a_1^2 \geq 0$, so

$$\frac{4\omega_1\sigma}{3\beta_2} \pm \frac{4\omega_1}{3\beta_2}\sqrt{\frac{\beta_1^2}{4\omega_1^2} + \frac{\zeta_2^2}{4} - \zeta_1^2} \geq 0. \quad (43)$$

That is

$$\sigma \geq \pm\sqrt{\frac{\beta_1^2}{4\omega_1^2} + \frac{\zeta_2^2}{4} - \zeta_1^2}, \quad (44)$$

where multiplying $\varepsilon$ at both sides of equation (44), and also considering that $\beta_1^2/4\omega_1^2$ is a smaller quantity, it gives that

$$\widehat{\zeta}_2 \leq 2\sqrt{(\varepsilon\sigma)^2 + \widehat{\zeta}_1^2}, \text{ that is } \widehat{\zeta}_{2\text{lim}} = 2\sqrt{(\varepsilon\sigma)^2 + \widehat{\zeta}_1^2}. \quad (45)$$

*3.4. The Critical Number.* When the structural parameters of the footbridge are fixed, in this case, the parameter vibration caused by the crowd movements, under the condition that certain number of pedestrians, that is, the parameter vibration for certain condition is reached, the parameter excitation of crowd can induce the large-scale lateral vibration of the footbridge. To meet stability, the conditions for walking on the Millennium Footbridge are shown as

$$\widehat{\zeta}_2 \leq \widehat{\zeta}_{2\text{lim}}. \quad (46)$$

According to Equations (45) and (46), it is indicated that

$$\frac{\lambda\alpha_{lv}m_p g}{\rho A + m_p} \leq 2\sqrt{(\varepsilon\sigma)^2 + \widehat{\zeta}_1^2}. \quad (47)$$

It is assumed that the pedestrians on the footbridge are evenly distributed, basically the same as the mass distribution law of the footbridge volume, and it is defined as

$$m_p L = \text{Nm}_{\text{ps}}, \quad (48)$$

where $N$ is the number of pedestrians on the footbridge, while the influence of crowd on damping of the footbridge is negligible. By virtue of Equations (47) and (48), it is indicated that

$$N \leq \frac{2L\rho A\sqrt{(\varepsilon\sigma)^2 + \widehat{\zeta}_1^2}}{\left(\lambda\alpha_{lv}g - 2\sqrt{(\varepsilon\sigma)^2 + \widehat{\zeta}_1^2}\right)m_{\text{ps}}}. \quad (49)$$

Figure 5 shows the relationship between the critical number of pedestrians and the parameter excitation frequency under different damping ratios. When $\varepsilon\sigma = 0$, if we change the damping ratio of the footbridge, according to the formula (49), we can get the corresponding critical number of pedestrians under six different damping ratios, 48, 122, 172, 251, 387, and 533, respectively. As the damping ratio increases, the critical number of pedestrians will increase as well. While the critical number of people has a linear relationship with the damping ratio, near the parametric resonance region, the damping ratio has a greater influence on the critical number of pedestrians than the nonparametric resonance region. The measured damping ratio of the Millennium Bridge is 0.007. The calculated critical number is 173, which is consistent with the measured critical number 178.

Where $\rho_{\text{plim}}$ is defined as the critical crowd density, the pedestrians are assumed to be uniformly distributed, the critical crowd density of the footbridge caused by the parameter vibration can be determined according to the measured parameter, so that it has a wider application for a similar type of footbridge. This parameter is related to the cross section of the footbridge, damping ratio, pedestrian synchronization coefficient, dynamic load coefficient, and pedestrian mass. When the relevant parameters of the bridge and pedestrians are known, the critical crowd density loaded by the footbridge can be obtained. The equation is shown as

$$\rho_{\text{plim}} = \frac{N}{\text{LB}} = \frac{2\rho A\widehat{\zeta}_1}{\left(\lambda\alpha_{lv}g - 2\widehat{\zeta}_1\right)\text{Bm}_{\text{ps}}}, \quad (50)$$

where $B$ is the effective walking width of the footbridge.

## 4. Nonlinear Parametric Vibration Model of the London Millennium Footbridge

Taking the mid-span of the London Millennium Footbridge as an example, we analyze the lateral nonlinear vibration

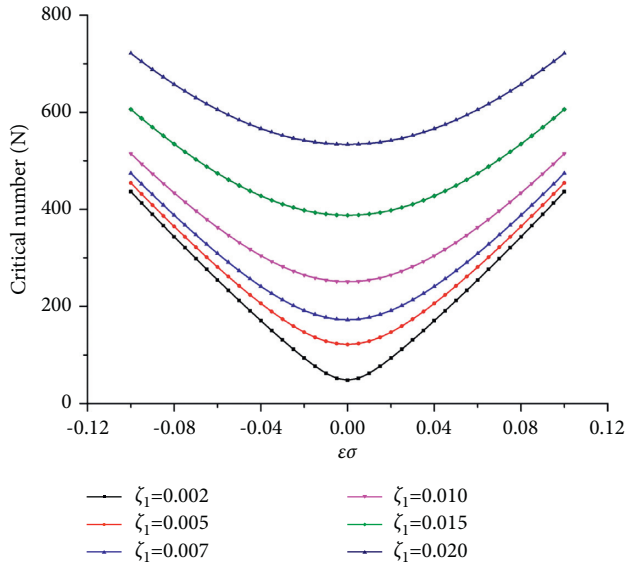


Figure 5: The relationship between critical number of pedestrians and pedestrian step frequency in different damping ratios.

parameters. The parameters employed in the calculation: the mass of the footbridge per unit length presents as $m_s$ = 2000kg/m; the average mass of a single pedestrian, that is, $m_{ps}$ = 70kg; the equivalent synchronized population ratio $\lambda = 0.3$, $\alpha_{l0} = 0.04$, and speed-related dynamic load factor is shown as $\alpha_{\mathrm{lv}} = 0.7$; the fixed first-order vibration frequency of the footbridge structure $f_{s1} = 0.48$ Hz, its span $L = 144$ m, and its equivalent bending stiffness $EI = 8.0383 \times 1010\ \mathrm{N{\cdot}m^2}$; The equivalent cross-sectional area $A = 0.2548\ \mathrm{m^2}$, and the equivalent compressive stiffness $EA = 5.3503 \times 1010\ \mathrm{N{\cdot}m^2}$.

### 4.1. Analysis of Vibration Parameters of the London Millennium Footbridge

*4.1.1. Amplitude Frequency Response Curve.* Figure 6 shows the amplitude-frequency response curve corresponding to different number of pedestrians when the damping ratio is 0.007. To be more specific, it can be seen from Figure 6 that different number of pedestrians corresponds to different response amplitudes; a large value is a stable solution, and a small value is nonstable solution. When the number of pedestrians is small, such as $N = 175$, the footbridge response has two close steady-state nontrivial solutions. As the number of pedestrians is getting larger and larger, the response amplitude varies with the excitation frequency under the same driving conditions. Because the horizontal first-order natural frequency of the Millennium Bridge is 0.48 Hz, when the excitation frequency of pedestrians walking is closer to 0.96 Hz, the parameter vibration of the Millennium Bridge will be excited. At this time, fewer pedestrians are required to cause a large lateral vibration of the Millennium Bridge. In the smaller range of crowd walking frequency close to 0.96 Hz, The Millennium Bridge will experience severe parametric vibrations.

As the number of people on the footbridge increases, the distance between each pair of resonance curves becomes larger, and there are jumps and lags in the parameter resonance response of the Millennium Footbridge. The resonance curve consists of a pair of nonintersecting curves. The resonance area is deviated to the right, and the amplitude-frequency curve appears as a hard spring. Furthermore, it can be found from Figure 6 that regarding the frequency tuning parameter $\sigma < 0$, there is only one equilibrium position; when the frequency tuning parameter is $\sigma > 0$, there are multiple equilibrium positions simultaneously.

Figure 7 presents the relationship between the number of pedestrians and lateral response amplitude of the footbridge when the damping ratio is 0.007. When the frequency of pedestrian excitation is twice that of the Millennium Footbridge (that is, $\omega_2 = 0.96$ Hz, $\sigma = 0$), a certain number of pedestrians N correspond to the lateral response of the footbridge, there is a stable nontrivial solution, and accordingly, a slight excitation can even induce a large vibration of the footbridge.

While the pedestrian walking frequency is less than 0.96 Hz, a certain number of pedestrians N corresponds to a stable nontrivial solution to the lateral response of the pedestrian bridge, and the smaller the excitation frequency, the more pedestrians are required to stimulate the Millennium Footbridge to vibrate; when the pedestrian frequency is greater than 0.96 Hz, there are two stable nontrivial solutions under the condition of a certain number of pedestrians N corresponding to a lateral response of the footbridge. Also, the number of pedestrians required to excite the vibration parameters of the Millennium Footbridge is independent of the excitation frequency. For the same number of pedestrians, the greater the excitation frequency is, the greater the response amplitude will be.

*4.1.2. Phase Angle of Movement by Pedestrians and the Footbridge.* Figure 8 indicated the relationship between phase angle and the mass ratio of pedestrian and bridge motion with different damping ratios. It can be seen from the data that as the mass ratio increases, the phase angle of pedestrian and bridge motion will slightly vary (increases or decreases), which can draw a conclusion that when the damping of the footbridge is certain, the measured phase angle according to the model is basically unchanged, approximately 90° or −90°.

*4.1.3. The Impact of the Number of People on the Bridge per Unit Time.* Affected by the purpose, location, and peak period of walking, the number of pedestrians on the footbridge in a unit time may be different, and different human flow will lead to different dynamic responses of the structure. Considering the total number of 250 people and the pedestrian numbers of 30, 50, 70, 90, and 110 at 400 s interval, the transverse dynamic response amplitude of Millennium Bridge is calculated.

It can be seen Figure 9 that, as the number of pedestrians on the footbridge increases per unit time, the dynamic response amplitude of the Millennium Footbridge decreases. This is because the fewer the pedestrians on the footbridge per unit time, the longer the hours pedestrians spend on the

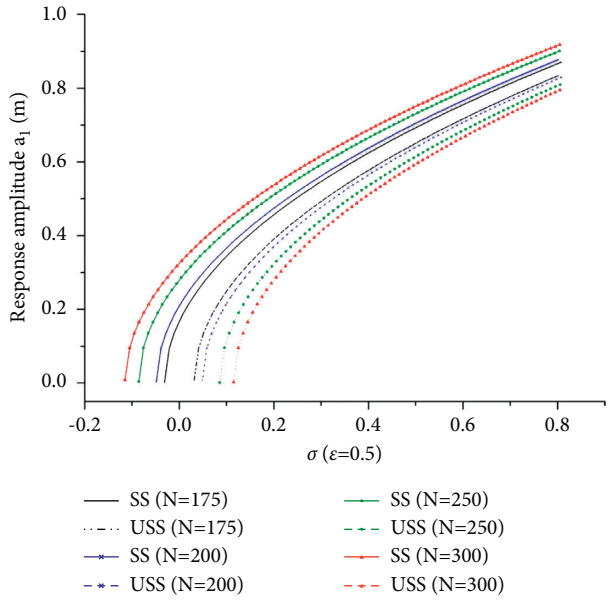


Figure 6: Amplitude frequency response curve ($\widehat{\zeta}_1 = 0.007$, $\varepsilon = 0.5$, SS: stable solution, USS: unstable solution).

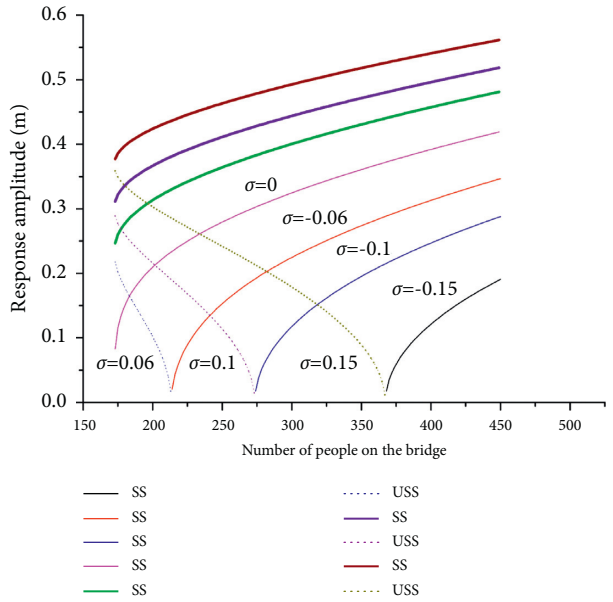


Figure 7: Curve of pedestrian number and lateral response amplitude of footbridge ($\widehat{\zeta}_1 = 0.007$, $\varepsilon = 0.5$, SS: stable solution, USS: unstable solution).

bridge. The easier it is to induce parameter resonance, when the number of pedestrians on the footbridge reaches 50 people/400 s, and the dynamic response of the structure will change slightly.

*4.1.4. The Influence of the Footbridge Structure Damping Ratio on Lateral Vibration.* In Figure 10, it takes 200 pedestrians on the footbridge as an example to calculate the dynamic response changes of the Millennium Footbridge under different damping ratios of the structure. It can be seen from the above figure that when the structural damping is considerably high, the lateral vibration response of the Millennium Footbridge will be smaller; while the structural damping is considerably low, the Millennium Footbridge undergoes parametric vibration, and its vibration response will increase sharply. When damping ratios of the structure are more than 0.01, 200 people are walking at the same time, the parametric vibration cannot be aroused, and the forced vibration is the main reason. Increasing the damping of the structure has no obvious effect on reducing the lateral vibration response. It can be seen from equation (38) that the amplitude of the footbridge parameter vibration caused by pedestrians increases as the resistance ratio of the footbridge decreases. It can be seen from equation (49) that the critical number of people decreases as the damping ratio of the footbridge increases. After the damping ratio of the pedestrian bridge structure makes the pedestrian bridge reach the critical condition of parametric vibration, if the damping ratio continues to decrease, it will cause a large lateral vibration of the pedestrian bridge, and the dynamic response amplitude caused by the forced vibration is smaller than the parametric vibration. The impact of the bridge damping ratio on the Millennium Bridge is different from that of the Japanese *T* bridge, because the vibration of the Millennium Bridge is mainly caused by parametric vibration, while in the case of the Japanese *T* bridge, it is resonance caused by forced vibration. Therefore, increasing the damping ratio of the Millennium Bridge can effectively avoid parametric vibration.

*4.1.5. Influence of Initial Conditions on Lateral Vibration.* Figure 11 shows the time-history diagram of the lateral displacement amplitude of the Millennium Footbridge under different initial conditions. It can be seen from the figure that when the parameters are in resonance, the initial conditions have no effect on the vibration amplitude in the final stable state. Generally, the initial displacement has no effect on vibration response, whereas the initial speed has a significant influence on the vibration response of the Millennium Footbridge. Furthermore, at the same initial displacement, the greater the initial speed is, the shorter is the time required to reach a stable vibration response.

*4.1.6. Effect of Synchronization Coefficient on Lateral Vibration.* Figure 12 presents the relationship between the critical number of pedestrians and synchronization coefficient under a certain damping ratio and parameter resonance. To be more specific, as the synchronization coefficient increases, the critical number of people decreases. In the case of a low synchronization coefficient, as the synchronization coefficient increases, the critical number of pedestrians decreases faster. When the synchronization coefficient reaches 0.5, the increase of the crowd synchronization coefficient will have little effect on the critical number of pedestrians.

*4.2. Numerical Analysis.* To rewrite equation (20) into the form of the following differential equations, it gives

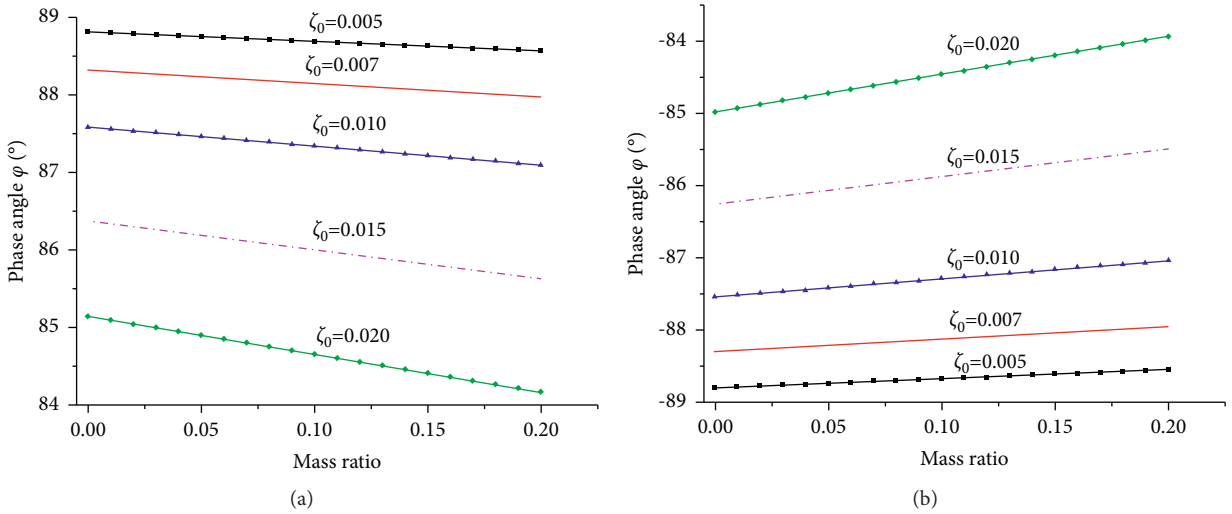


Figure 8: The relationship between phase angle and mass ratio of pedestrian and bridge motions under different damping ratios. (a) Positive phase angle. (b) Negative phase angle.

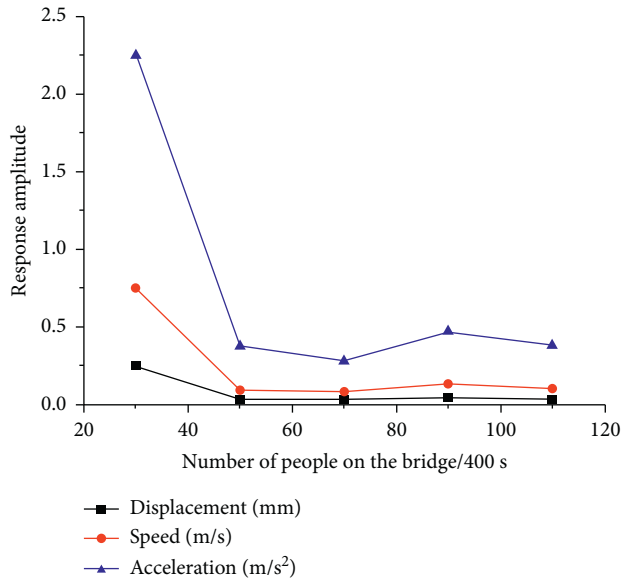


Figure 9: The relationship between dynamic response amplitude and the number of pedestrians on the Millennium Footbridge.

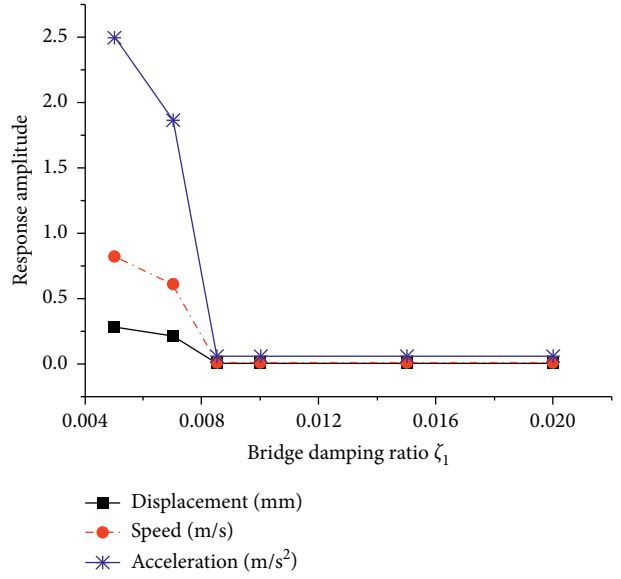


Figure 10: The relationship between lateral response amplitude of the Millennium Footbridge and damping ratio.

$$\begin{cases} \dot{w}_1(t) = v_1(t), \\ \dot{v}_1(t) = -\varepsilon\zeta_1 v_1(t) + \varepsilon\zeta_2 \cos\left(\omega_p t\right) v_1(t) - \omega_1^2 w_1(t) \\ + \varepsilon\beta_1 \cos\left(\omega_p t\right) w_1(t) - \varepsilon\beta_2 w_1^3(t) \\ + \varepsilon F_0 \cos\left(\omega_p t\right). \end{cases} \tag{51}$$

The paper introduces MATLAB language; further, the fourth-order Runge–Kutta method is used to get the second-order nonlinear vibration differential, equation (51). The purpose is to provide a specific solution by the built-in function ODE45 of MATLAB. Figure 13 shows the London Millennium Footbridge time history curve of lateral vibration displacement, lateral vibration velocity, and lateral vibration acceleration when there are 50 pedestrians, 120 pedestrians, 175 pedestrians, and 250 pedestrians crossing the footbridge. In this way, the initial displacement is 0.001 m and the initial speed is 0.001 m/s, while the damping ratio is the measured value 0.007.

It is worth calling attention to the fact that parametric vibration cannot be excited in the case of small number of pedestrians, generally forced vibration. Accordingly, the vibration response is an equal period response, as shown in panels (a) and (b) in Figure 13. The time history curve decays first and then vibrates at a constant amplitude; when the number of pedestrians is around 175, the corresponding parameter vibration is excited. And, the time history curve diverges slowly, as shown in Figure 13(c). When the number of pedestrians exceeds the critical number of people, it is

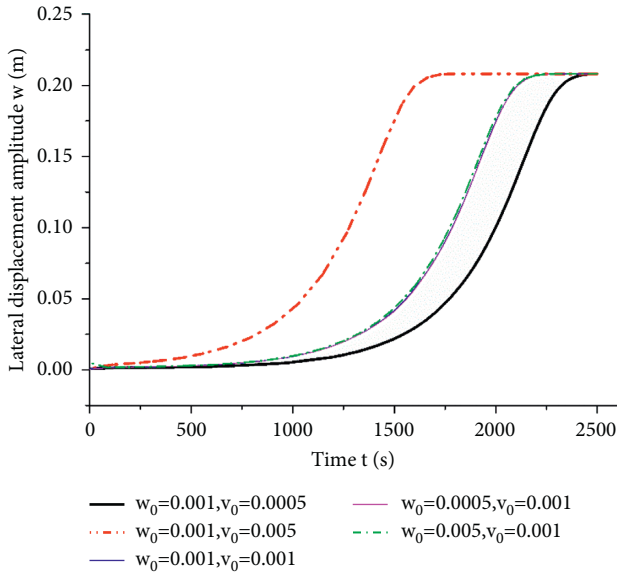


Figure 11: Time history diagram of lateral displacement amplitude under different initial conditions.

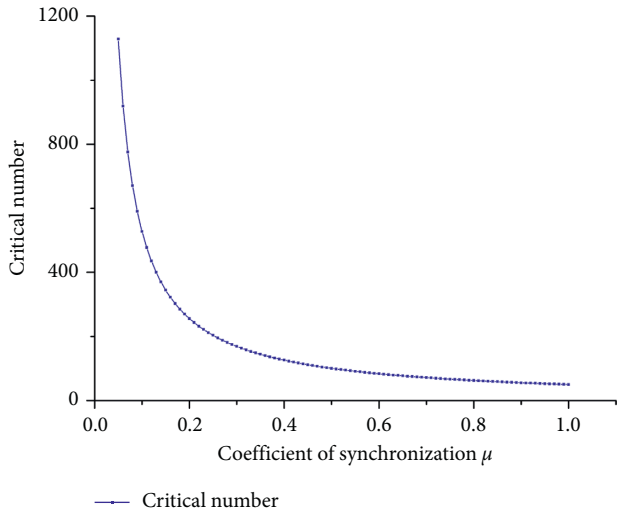


Figure 12: The relationship between critical number of pedestrians and synchronization coefficient under parametric resonance.

possible that the parameter vibration is obvious, even with a little disturbance. A large parametric vibration is aroused faster, this is largely due to parametric vibration control, and the time history curve diverges faster, which is consistent with the phenomenon actually observed on the spot, and the more pedestrians on the footbridge, the faster the vibration response changes; see Figure 13(d). The lateral displacement will be enlarged continually when the Np = 175. Since the author considered the influence of nonlinearity in the model, the lateral displacement becomes constant when the time reaches 5000 s. However, even assuming that the force of the crowd on the pedestrian bridge is linear with the bridge vibration speed, lateral displacement of the structure will not be enlarged continually when the Np = 250, so the vibration response tends to be stable at 700 s.

*4.3. Simulation Analysis of the Pedestrian Boarding Process of the London Millennium Footbridge Experiment.* Assuming that the number of pedestrians on the bridge increases by 50 every 400 s, and by 2000 s, the number of pedestrians increases to 250. Figures 14–17 present the number of pedestrians on the footbridge, the time history curve of mid-span displacement, the time history curve of mid-span speed, and medium acceleration time history curve, respectively. By 2000 s, the maximum displacement amplitude reaches 37 mm, while the maximum velocity is 0.11 m/s, and the maximum acceleration is 0.33 m/s$^2$. Among them, it can be observed that the calculated speed value is close to the test value, accordingly the test speed is 0.135 m/s, which shows that the numerical simulation has high reliability and the parameter values are more reasonable. From Figures 14–17, it was found that before the number of pedestrians on the footbridge reaches the critical number of persons, the footbridge's response is small; in addition, the change of response is not obvious. When the number of people on the footbridge exceeds the critical number of people, the bridge's response rapidly increases. In other words, when the number of persons on the Millennium Footbridge reaches the critical value, its lateral amplitude reaches the critical value, which causes the lateral vibration response to increase rapidly. Figures 15–17 show that the vibration responses will continually increase; however, since the author considered the influence of nonlinearity in the model, they will become constant after 2400 s when the Np = 250. In this experiment, the vibration model accounts for the great vibration of mid-span on the London Millennium Footbridge.

## 5. Nonlinear Parametric Vibration Analysis of the Footbridges considering the Time-Lag Effect

In the process of pedestrians' movement, the force exerted by pedestrians on the footbridge cannot be immediately reflected on the pedestrian bridge, and there is a time lag, which is the phenomenon of time lag. In this article, the focus is on the three major causes of time lag. One is the impact of pedestrians' own factors, that is, the time that persons need to respond; the other cause is the contact between pedestrians and the footbridge, and the pace of pedestrian adjustment and footbridge vibration cannot be achieved simultaneously. In addition, the third cause is regarded as parameters of the footbridge itself, such as the classification, span, quality, stiffness, feature, and thickness of the footbridge. Investigation shows that the thinner and harder the contact material between the pedestrian and the bridge deck, the smaller the time lag [24, 25]. The current research on time lag basically focuses on the application of time lag phenomenon for vibration reduction control. It is therefore concluded that the time lag phenomenon can help reduce vibration of the structure, and change stability and bifurcation behavior of linear and nonlinear vibration of the structure [26–31]. However, there are few researches reported on the time lag phenomenon in the human-induced bridge vibration. The Nakamura model was used by Lin and

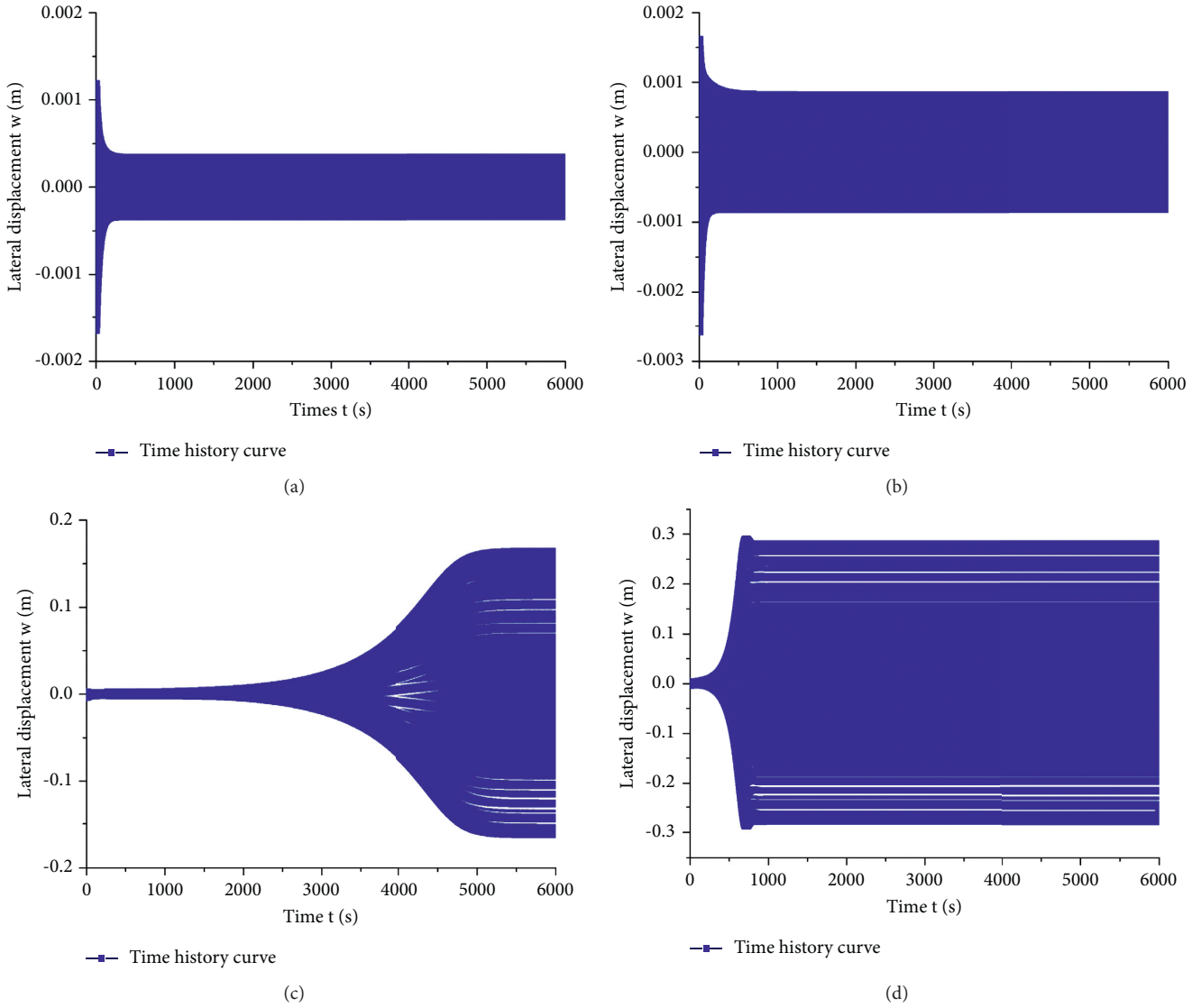


Figure 13: Time history curve of mid-span displacement with different number of pedestrians on the footbridge. (a) $N_p = 50$. (b) $N_p = 120$. (c) $N_p = 50$. (d) $N_p = 120$.

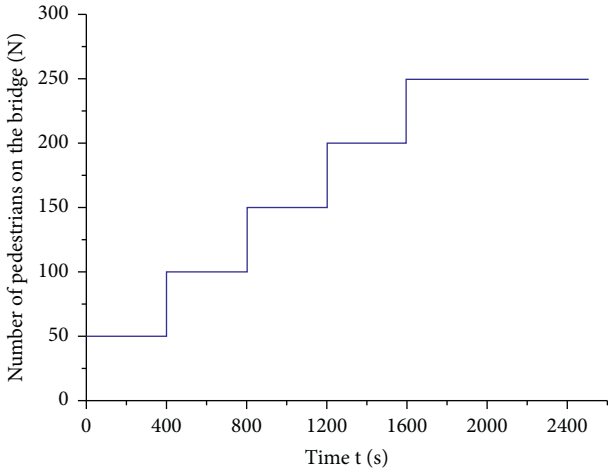


Figure 14: The number of pedestrians on the footbridge.

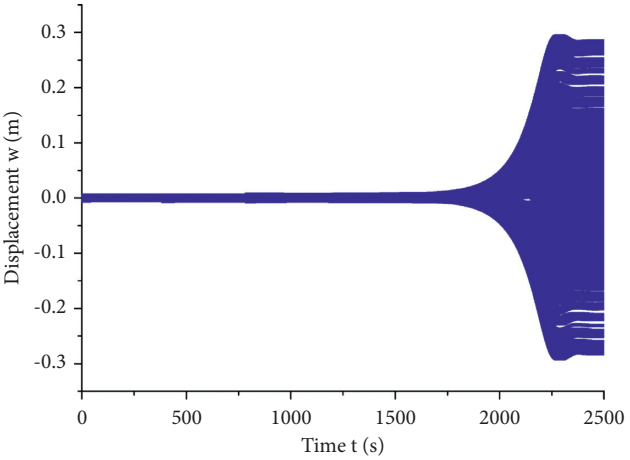


Figure 15: Time history curve of mid-span displacement.

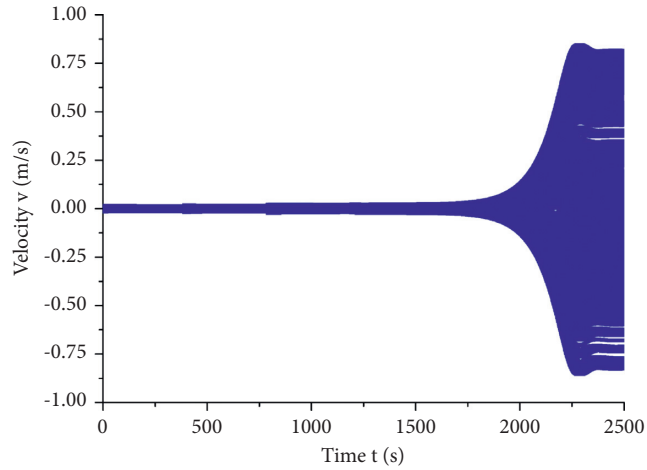


Figure 16: Midspan velocity time history curve.

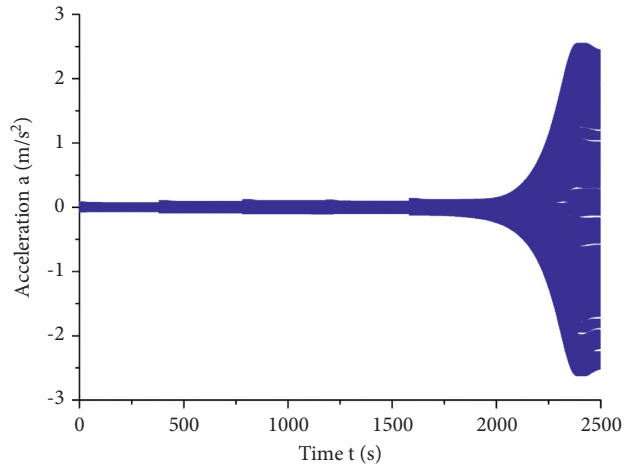


Figure 17: Time history curve of mid-span acceleration.

Zhen to analyze the time lag in the forced vibration, which will help reduce vibration of the footbridge [24, 25]. Hence, it is of great significance to analyze the influence of time lag on the vibration of bridge parameters caused by pedestrians.

*5.1. Nonlinear Parametric Vibration Theory considering the Time-Delay Effect.* On the basis of the nonlinear parametric vibration model of the footbridges derived previously, the time-lag effect is introduced to analyze and investigate the impact of time lag on the parametric vibration of the footbridges. Omitting the longitudinal effect, the nonlinear vibration equation of lateral parameters in consideration of time lag phenomenon can be expressed as

$$\begin{aligned}&\ddot{w}_1(t) + \varepsilon\zeta_1\dot{w}_1(t) - \varepsilon\zeta_2\cos\left(\omega_p(t-\tau)\right)\dot{w}_1(t-\tau)\\&\quad + \omega_1^2 w_1(t) + \varepsilon\beta_2 w_1^3(t) - \varepsilon F_0\cos\left(\omega_p(t-\tau)\right) = 0.\end{aligned} \tag{52}$$

Multi-scale approach is applied to solve equation (52); the first approximate solution of equation (52) now gives

$$w_{11}(t) = u_0(T_0, T_1) + \varepsilon u_1(T_0, T_1), \tag{53}$$

$$w_{11\tau}(t) = u_{0\tau}(T_0, T_1) + \varepsilon u_{1\tau}(T_0, T_1). \tag{54}$$

Substituting equations (23), (24), (53), and (54) into (52), assuming that the coefficients of the small parameters $\varepsilon$ on both sides of the equation is equal, the linear partial differential equation reads as follows

$$\varepsilon^0:\ D_0^2 u_0 + \omega_1^2 u_0 = 0, \tag{55}$$

$$\begin{aligned}\varepsilon^1:\ D_0^2 u_1 + \omega_1^2 u_1 &= -2D_0D_1u_0 - \mu_1 D_0 u_0\\&\quad + \mu_2 D_0 u_{0\tau}\cos\left(\omega_p(t-\tau)\right) - \beta_2 u_0^3\\&\quad + F_0\cos\left(\omega_p(t-\tau)\right).\end{aligned} \tag{56}$$

Therefore, to assume the solution of equation (55), it gives

$$u_0(T_0, T_1) = A(T_1)e^{j\omega_1 T_0} + \overline{A}(T_1)e^{-j\omega_1 T_0}. \tag{57}$$

The time lag is presented as

$$u_{0\tau}(T_0, T_1) = A_\tau(T_1)e^{j\omega_1(T_0-\tau)} + \overline{A}_\tau(T_1)e^{-j\omega_1(T_0-\tau)}. \tag{58}$$

Rewriting $\mu_2 D_0 u_{0\tau}\cos(\omega_p(t-\tau))$ and $F_0\cos(\omega_p(t-\tau))$ into plural form, and further substituting equation (57) and (58) into (56) leads to

$$\begin{aligned} D_0^2 u_1 + \omega_1^2 u_1 = &-(2D_1 A j\omega_1 + \mu_1 A j\omega_1)e^{j\omega_1 T_0} \\ &+ \frac{\mu_2 j\omega_1}{2}\left(A_\tau e^{j(\omega_p+\omega_1)(T_0-\tau)} - \overline{A}_\tau e^{j(\omega_p-\omega_1)(T_0-\tau)}\right) \\ &- \beta_2\left(A^3 e^{3j\omega_1 T_0} + 3A^2\overline{A}e^{j\omega_1 T_0}\right) \\ &+ \frac{F_0}{2}e^{j(\omega_p T_0 - \omega_p\tau)} + \text{cc}. \end{aligned} \tag{59}$$

In which, cc is regarded as the conjugate complex number of the previous expression. From equation (60), it can be found that the time system has parametric vibration when $\omega_p = 2\omega_1$, and the time system is forced vibration when $\omega_p = 2\omega_1$. It is likely for the pedestrians' lateral force to simultaneously appear 1 : 2 parametric resonance and 1 : 1 forced vibration. To state more clearly, the following part is devoted to analyze 1 : 2 parametric vibration considering the time-lag effect, and also to study the impact of time lag on the footbridge vibration.

Inserting new excitation frequency tuning parameters, it reads

$$\omega_p = 2\omega_1 + \varepsilon\sigma. \tag{60}$$

Based on equation (59), the condition for eliminating the permanent term can be obtained

$$\begin{aligned} &2D_1 A j\omega_1 + \mu A j\omega_1 + \frac{\mu_2 j\omega_1}{2}\overline{A}_\tau e^{j\sigma T_1}e^{-j(\omega_1+\varepsilon\sigma)\tau} \\ &\quad + 3\beta_2 A^2\overline{A} = 0. \end{aligned} \tag{61}$$

For the lateral vibration of the footbridge caused by pedestrians, the time lag $\tau$ is not obviously large. Whereas, in the case of small value $\varepsilon$, according to the Taylor series, $\overline{A}_\tau$ and $A_\tau$ can be defined as

$$\begin{aligned} \overline{A}_\tau(T_1) &= \overline{A}_\tau(\varepsilon t) = \overline{A}(\varepsilon t - \varepsilon\tau) = \overline{A}(T_1 - \varepsilon\tau) \\ &= \overline{A}(T_1) - \varepsilon\tau\overline{A}'(T_1) + \frac{1}{2}\varepsilon^2\tau^2\overline{A}''(T_1) \approx \overline{A}(T_1). \end{aligned} \tag{62}$$

Hence, the equation can be written as

$$\begin{aligned} &2D_1 A j\omega_1 + \mu A j\omega_1 + \frac{\mu_2 j\omega_1}{2}\overline{A}(T_1)e^{j\sigma T_1}e^{-j(\omega_1+\varepsilon\sigma)\tau} \\ &\quad + 3\beta_2 A^2\overline{A} = 0, \end{aligned} \tag{63}$$

$A(T_1)$ is written into exponential form, and it gives

$$A(T_1) = \frac{a_1(T_1)}{2}e^{j\gamma_1(T_1)}. \tag{64}$$

Substituting equations (64) into (63), comparing its real part and imaginary part, and assuming $\psi = \sigma T_1 - 2\gamma_1$, it can be found:

$$\begin{aligned} D_1 a_1 &= -\frac{\zeta_1 a_1}{2} - \frac{\zeta_2 a_1}{4}\cos\varphi\cos((\omega_1+\varepsilon\sigma)\tau) \\ &\quad - \frac{\zeta_2 a_1}{4}\sin\varphi\sin((\omega_1+\varepsilon\sigma)\tau), \\ D_1\varphi_1 &= \sigma + \frac{\zeta_2}{2}\sin\varphi\cos((\omega_1+\varepsilon\sigma)\tau) \\ &\quad - \frac{\zeta_2}{2}\cos\varphi\sin((\omega_1+\varepsilon\sigma)\tau) - \frac{3\beta_2 a_1^2}{4\omega_1}. \end{aligned} \tag{65}$$

Furthermore, with the fixed value of $D_1 a_1 = 0$, $D_1\varphi_1 = 0$, it reads

$$\begin{aligned} \frac{\zeta_1 a_1}{2} &= -\frac{\zeta_2 a_1}{4}\cos\varphi\cos((\omega_1+\varepsilon\sigma)\tau) \\ &\quad - \frac{\zeta_2 a_1}{4}\sin\varphi\sin((\omega_1+\varepsilon\sigma)\tau), \end{aligned} \tag{66}$$

$$\begin{aligned} \sigma - \frac{3\beta_2 a_1^2}{4\omega_1} &= \frac{\zeta_2}{2}\cos\varphi\sin((\omega_1+\varepsilon\sigma)\tau) \\ &\quad - \frac{\zeta_2}{2}\sin\varphi\cos((\omega_1+\varepsilon\sigma)\tau). \end{aligned} \tag{67}$$

Equations (66) and (67) are squared and added, and therefore,

$$\zeta_1^2 + \left(\sigma - \frac{3\beta_2 a_1^2}{4\omega_1}\right)^2 = \frac{\zeta_2^2}{4}. \tag{68}$$

Equation (68) is the amplitude-frequency curve of nonlinear parametric vibration considering the time-lag effect. Compared equation (36) with (68), in virtue of the small value of $\beta_1$. In the nonlinear parametric vibration of

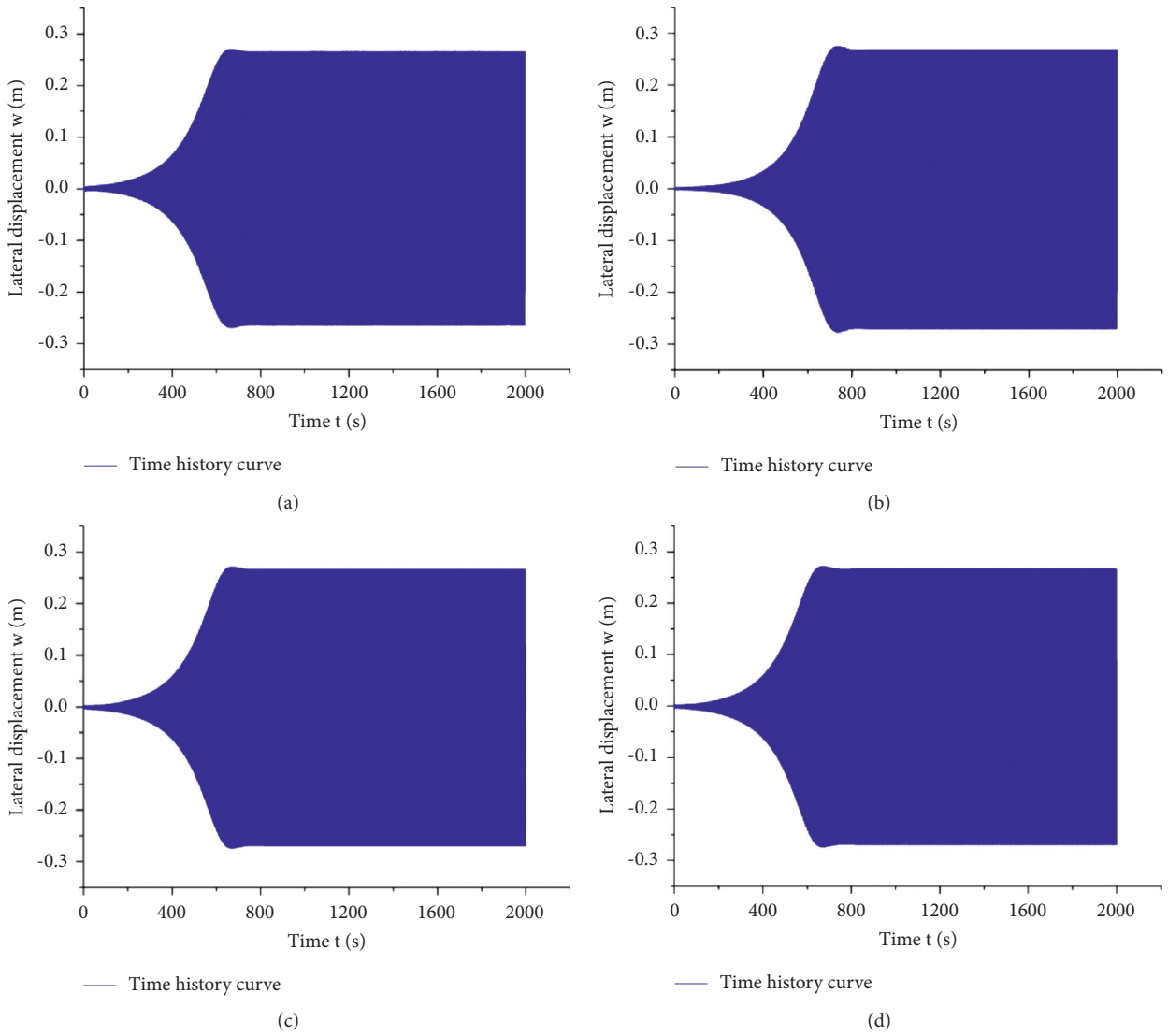


Figure 18: Lateral displacement in various conditions. (a) $r = 0.2$. (b) $r = 0.5$. (c) $r = 1.0$. (d) 2.0.

the Millennium Bridge, the time lag has no effect on amplitude of the structure.

*5.2. Numerical Analysis.* Taking 250 people on the Millennium Bridge as an example, the time history analysis of the parameter vibration of the Millennium Bridge considering the time lag is carried out. Figure 18 shows the time history curve of displacement response considering the time lag and the initial conditions.

It is generally observed that Figure 18 indicates the lateral vibration displacement of the London Millennium Footbridge in case of different time lags. Comparing Figures 9 and 18, it can be concluded that the response amplitude of the Millennium Footbridge does not vary with the existence of the time-lag effect and the time lag, which is consistent with the theoretical approximation solution. The structural vibration response obtained is similar to the actual measurement regardless of considering or without considering the time delay. Accordingly, the critical number of pedestrians obtained is also the same, which proves that theoretical analysis is correct.

However, when the time lag $\tau$ takes different values, the time required to reach the peak value and the stable amplitude will vary without any obvious principles, reflecting the fact that the time lag has a complicated influence on the time needed to reach the peak value and stable amplitude. This is because in parametric vibration, the response of the structure depends on the time variable. Even if there is time-lag effect, its influence on the amplitude can be coved as the change of time. It is worth calling attention to the fact that it is the difference between parametric vibration and forced vibration.

## 6. Conclusions

This paper takes the London Millennium Footbridge as an example, considering the influence of pedestrian quality on the frequency of footbridges. A detailed nonlinear transverse

parametric vibration model is proposed in consideration of the relationship between force and speed. Using Galerkin and multi-scale perturbation approach, the investigation also analyzes the large-scale vibration caused by the combination of human-induced footbridge parametric vibration and forced vibration. After the experiment on the causes of the large-scale vibration phenomenon of the Millennium Footbridge, the following conclusions can be drawn:

(1) This model can better and further explain that, when the fundamental frequency of the Millennium Footbridge is far away from the pedestrians' lateral walking frequency, still large lateral vibrations will occur. In additionally, the theoretical calculation of the critical number of pedestrians is close to the measured value, indicating that the established model has a considerably high reliability.

(2) The closer the walking frequency is to two times the natural frequency of the footbridge, the smaller the number of pedestrians required to excite large vibrations. As long as a slight excitation, the pedestrian bridge will also vibrate significantly.

(3) When the structural damping is relatively low, the Millennium Footbridge undergoes parametric vibration, and the vibration response increases sharply; when the parametric resonance occurs, the initial conditions have no effect on the vibration amplitude in the final steady state; as the synchronization coefficient increases, the critical number of pedestrians decreases.

(4) As for the Footbridge parameters with regard to vibration caused by pedestrians, when only considering the lag of pedestrians' force on the footbridge, the time-lag effect has no effect on the amplitude, but has an effect on the time needed to reach a stable amplitude [32].

## Data Availability

The data used to support the findings of this study are available from the corresponding author upon request.

## Conflicts of Interest

The authors declare that they have no conflicts of interest.

## Authors' Contributions

Zhou Chen was responsible for data curation, formal analysis, investigation, methodology, software, visualization, and writing—review and editing. Hongxin Lin was concerned with data curation, software, and writing—review, editing, and drawing. Dengyuan Deng was involved in project administration and validation. Wanjie Xu was responsible for writing and language. Hanwen Lu looked into formal analysis, investigation, methodology, and funding acquisition. Zepeng Chen wrote the original draft.

## Acknowledgments

This work was financially supported by the National Natural Science Foundation of China (Grant nos. 51908146 and 52008109) and the Foshan self-funded science and technology plan project (Grant no. 1920001001539).

This paper is an extended version of the paper "Study on nonlinear parametric vibration of footbridge considering time-lag effect, doi:10.1088/1757-899X/490/3/032016."

## References

[1] S.-i. Nakamura and T. Kawasaki, "Lateral vibration of footbridges by synchronous walking," *Journal of Constructional Steel Research*, vol. 62, no. 11, pp. 1148–1160, 2006.

[2] B. Jia, X. Yu, Q. Yan, Z. Yang, and Y. Chen, "Stability analysis of pedestrian-induced large lateral vibration on a footbridge," *Structure and Infrastructure Engineering*, vol. 17, no. 3, pp. 291–301, 2020.

[3] A. N. Blekherman, "Swaying of pedestrian bridges," *Journal of Bridge Engineering*, vol. 10, no. 2, pp. 142–150, 2005.

[4] A. N. Blekherman, "Autoparametric resonance in a pedestrian steel arch bridge: solferino bridge, Paris," *Journal of Bridge Engineering*, vol. 12, no. 6, pp. 669–676, 2007.

[5] H. Han, D. Zhou, T. Ji, and J. Zhang, "Modelling of lateral forces generated by pedestrians walking across footbridges," *Applied Mathematical Modelling*, vol. 89, pp. 1775–1791, 2021.

[6] K. Van Nimmen, G. Lombaert, G. Van den Broeck, and P. Broeck, "The impact of vertical human-structure interaction on the response of footbridges to pedestrian excitation," *Journal of Sound and Vibration*, vol. 402, pp. 104–121, 2017.

[7] G. M. Maria, L. Eleonora, and L. Giulia, "Coupled analysis of footbridge-pedestrian dynamic interaction," *Engineering Structures*, vol. 176, pp. 127–142, 2018.

[8] M. Bocian, J. H. G. Macdonald, and J. F. Burn, "Probabilistic criteria for lateral dynamic stability of bridges under crowd loading," *Computers & Structures*, vol. 136, pp. 108–119, 2014.

[9] X. Su, H. Kang, J. Chen, T. Guo, C. Sun, and Y. Zhao, "Experimental study on in-plane nonlinear vibrations of the cable-stayed bridge," *Nonlinear Dynamics*, vol. 98, no. 2, pp. 1247–1266, 2019.

[10] J. Peng, M. J. Xiang, L. H. Wang, and X. Z. Xie, "Nonlinear primary resonance in vibration control of cable-stayed beam with time delay feedback," *Mechanical Systems and Signal Processing*, vol. 137, 2020.

[11] C. S. Sun, Y. B. Zhao, Z. Q. Wang, and J. Peng, "Effects of longitudinal girder vibration on non-linear cable responses in cable-stayed bridges," *European Journal of Environmental and Civil Engineering*, vol. 21, no. 1, pp. 1–14, 2015.

[12] Y. Fujino, B. M. Pacheco, S.-I. Nakamura, and P. Warnitchai, "Synchronization of human walking observed during lateral vibration of a congested pedestrian bridge," *Earthquake Engineering & Structural Dynamics*, vol. 22, no. 9, pp. 741–758, 1993.

[13] E. T. Ingólfsson, C. T. Georgakis, and J. Jönsson, "Pedestrian-induced lateral vibrations of footbridges: a literature review," *Engineering Structures*, vol. 45, no. 15, pp. 21–52, 2012.

[14] M. W, J. Brownjohn, P. Fok, M. Roche, and P. Omenzetter, "Long span steel pedestrian bridge at Singapore Changi Airport–part 2:Crowd loading tests and vibration mitigation measures," *Structural Engineer*, vol. 82, no. 16, pp. 28–34, 2004.

[15] J. Xiong, J. Chen, and C. Caprani, "Spectral analysis of human-structure interaction during crowd jumpings," *Applied Mathematical Modelling*, vol. 89, pp. 610–626, 2020.
[16] P. Dallard, T. Fitzpatrick, A. Flint, S. L. Bourva, and M. Willford, "The london millennium footbridge," *Structural Engineer*, vol. 79, no. 171, pp. 17–33, 2001.
[17] G. Piccardo and F. Tubino, "Parametric resonance of flexible footbridge under crowd-induced lateral vibration," *Journal of Sound and Vibration*, vol. 311, no. 1-2, pp. 353–371, 2008.
[18] L. Ouyang, B. Ding, T. Li, B. Zhen, and S. Caddemi, "A suspension footbridge model under crowd-induced lateral excitation," *Shock and Vibration*, vol. 2019, pp. 1–11, 2019.
[19] J. P. Wang and J. Chen, "A comparative study on different walking load models," *Structural Engineering & Mechanics*, vol. 63, no. 6, pp. 847–856, 2017.
[20] E. Bassoli, P. Gambarelli, and L. Vincenzi, "Human-induced vibrations of a curved cable-stayed footbridge," *Journal of Constructional Steel Research*, vol. 146, pp. 84–96, 2018.
[21] A. T. Marcelo and M. G. Herbert, "A coupled biodynamic model for crowd-footbridge interaction," *Engineering Structures*, vol. 177, pp. 47–60, 2018.
[22] H. Y. Hu, *Applied Nonlinear Dynamics*, Aviation industry press, Beijing, 2000.
[23] HiVoSS (Human induced Vibrations of Steel Structures), Design of Footbridges-Background Document, 2008.
[24] P. Dallard, T. Fitzpatrick, A. Flint et al., "London millennium bridge: pedestrian-induced lateral vibration," *Journal of Bridge Engineering*, vol. 6, no. 6, pp. 412–417, 2001.
[25] R. Lin, B. Zhen, and Z. Y. Ren, "Calculation for the critical number of pedestrians on a footbridge by using the modified nakamura's model," *Applied Mechanics and Materials*, vol. 427-429, pp. 408–411, 2013.
[26] B. Zhen, W. K. Wong, J. Xu, and W. Xie, "Application of nakamura's model to describe the delayed increase in lateral vibration of footbridges," *Journal of Engineering Mechanics*, vol. 139, no. 12, pp. 1708–1713, 2013.
[27] Y. Tang, J. Peng, L. Li, and H. Sun, "Nonlinear vibration mitigation of a beam excited by moving load with time-delayed velocity and acceleration feedback," *Applied Sciences*, vol. 10, no. 11, p. 3685, 2020.
[28] F. An, W.-d. Chen, and M.-q. Shao, "Dynamic behavior of time-delayed acceleration feedback controller for active vibration control of flexible structures," *Journal of Sound and Vibration*, vol. 333, no. 20, pp. 4789–4809, 2014.
[29] F. An, W.-d. Chen, and M.-q. Shao, "Study on discrete acceleration feedback control with time delay," *Journal of Vibration and Control*, vol. 21, no. 7, pp. 1267–1285, 2015.
[30] L. Zhang, H. Wang, and H. Hu, "Global view of Hopf bifurcations of a van der Pol oscillator with delayed state feedback," *Science China Technological Sciences*, vol. 53, no. 3, pp. 595–607, 2010.
[31] J. Peng, M. J. Xiang, L. X. Li, and H. X. Sun, "Time-delayed feedback control of piezoelectric elastic beams under superharmonic and subharmonic excitations," *Applied Sciences*, vol. 9, no. 8, p. 1157, 2019.
[32] S. Ma, Q. Lu, and Z. Feng, "Double Hopf bifurcation for van der Pol-Duffing oscillator with parametric delay feedback control," *Journal of Mathematical Analysis and Applications*, vol. 338, no. 2, pp. 993–1007, 2008.